

The eLoaD platform endows centrifugal microfluidics with on-disc power and communication

Saraí M. Torres Delgado^{a,b}, Jan G. Korvink^b, Dario Mager^{b,*}

^aLaboratory for Simulation, Department of Microsystems Engineering (IMTEK), University of Freiburg, Georges-Koehler-Allee 103, Freiburg im Breisgau 79110, Germany.

^bInstitute of Microstructure Technology, Karlsruhe Institute of Technology, Hermann-von-Helmholtz-Platz 1, Eggenstein-Leopoldshafen 76344, Germany.

Abstract

In this paper we present a comprehensive description of the design, fabrication and operation of an electrified Lab-on-a-Disc (eLoaD) system. The smart platform is developed to extend conventional Lab-on-a-Disc applications with an electronic interface, providing additional flow control and sensing capabilities to centrifugal microfluidics platforms. Wireless power is transferred from a Qi-compliant transmitter to the eLoaD platform during rotation. An Arduino-based microcontroller, a Bluetooth communication module, and an on-board SD-card are integrated into the platform. This generalises the applicability of the eLoaD and its modules for performing a wide range of laboratory unit operations, procedures, or diagnostic assays, all controlled wirelessly during spinning. The lightweight platform is fully reusable and modular in design and construction. An interchangeable and non-disposable application disc is fitted with the necessary sensors and/or actuators for a specific assay or experiment to be performed. A particular advantage is the ability to continuously monitor and interact with LoaD experiments, overcoming the limitations of stroboscopy. We demonstrate the applicability of the platform for two sensing experiments involving optical, electrochemical, and temperature detection, and one actuation experiment involving controlled heating/cooling, and flow control with active valves. The complete electronic designs and example programming codes are extensively documented in the supplementary material for easy adaptation.

Keywords: Wireless, Lab-on-a-Disc, centrifugal platform, automation, on-disc

1. Introduction and motivation

Lab-on-a-chip (LOC) systems are portable devices designed and developed for complex diagnostic purposes. They integrate basic analytic steps such as sample and reagent injection, mixing, sedimentation, amplification, incubation, and detection. Lab-on-a-Disc systems form a sub-category in the form of a spinning microfluidic disc, typically of the same dimensions as a common optical disc such as a CD or DVD, in which the centrifugal force is used to pump liquids along radial microfluidic channels. The system is particularly advantageous for use in ‘point-of-care’ and ‘point-of-use’ applications, as its function requires only a common spindle motor rather than specialist microfluidic pumps. Laboratory unit operations (LUOs) such as valving, pumping, metering, mixing, and sample preparation on centrifugal microfluidic platforms have been widely studied (Ducrée et al., 2007; Strohmeier et al., 2015; Kong et al., 2016). Sample preparation might include a single or multiple steps such as particle sorting, purification/concentration, sedimentation/filtration, and cell lysis. The platform is particularly powerful due to the inherent ability to centrifuge samples, such as needed for blood processing (Kinahan et al., 2016b). The existing solutions to perform these LUOs have been mainly achieved using passive techniques.

However, while the LoaD technique has simplified basic operations, solutions to other arising needs, such as the integration of (active) operations, or the readout of a bioassay result, has proven more challenging to achieve when the platform is under continuous spinning motion. Without the possibility of a direct connection of sensors and/or actuators to a stationary power supply, stroboscopic observation and excitation has remained the most widely means of detection and actuation in LoaD systems (Burger et al., 2016). These include absorbance (colorimetric), fluorescence and chemiluminescence detection methods for many biological and chemical assays, as well as laser scanning microscope systems, imaging based detectors. Even resonance detection via vibration and deflection sensing techniques for mechanical (cantilever-based) sensors have been reported (Burger et al., 2016; Kong et al., 2016).

* Corresponding author: dario.mager@kit.edu

Optical elements are not only used within detection schemes, but can also actuate, for example to initiate valving mechanisms while melting paraffin wax plugs (Park et al., 2007; Garcia-Cordero et al., 2010; Abi-Samra et al., 2011), or as heat source for thermocycle amplification (Burger et al., 2011; Focus Diagnostics, 2016; Brennan et al., 2017). The eminent use of optical elements is even more evident when considering commercially available microfluidic centrifugal systems (Strohmeier et al., 2015), many of which (Abaxis, 2018; LaMotte, 2018; Samsung, 2017; Focus Diagnostics, 2016; Skyla, 2018; Biosurfit, 2018; GenePOC, 2018; SpinChip Diagnostics AS, 2018) are either purely passive, and/or employ active optical methods. Some case studies include semi-active mechanisms such as magnets, which of course do not require a power supply on the disc.

From the literature we therefore observe that the LoaD community has opted for indirect (off-disc and therefore non-contact) and non continuous sensing and actuation solutions that have direct power and data connection lines, rather than implementing direct contact and continuous sensing and actuation with indirect (wireless) power and data connections.

Our second observation is that, in many instances, a microfluidic disc is required to be placed in direct contact with sensors and/or actuators that themselves are directly connected to benchtop equipment and/or to a power supply. This implies that the microfluidic disc is to be stopped and aligned for a few seconds or even minutes (Noroozi et al., 2011; Amasia et al., 2012; Li et al., 2013; Nwankire et al., 2015). A spin-stop solution can result in undesired delays for time-sensitive experiments, or worse, alter results due to a deceleration in the reaction taking place.

A reason for these conventions might be that LoaD originated out of the idea of using a CD-player for actuation and read-out purposes, in which a stationary laser reads data directly from the spinning disc. Over the years many LUOs have been developed that allowed most tests to be performed (Strohmeier et al., 2015) in this setting, reducing the need to make fundamental changes to the sensing and actuation principles.

There have been a few pioneer publications reporting on centrifugal microfluidic systems in which power is transferred to the spinning platform, such as by using slip-rings (Cho et al., 1982; Martinez-Duarte et al., 2010; Abi-Samra et al., 2013; Kim et al., 2013; Andreasen et al., 2015), or even wirelessly (Burger et al., 2011; Wang et al., 2013), allowing the mounting of electric components in direct contact with the microfluidic disc without the need of stopping it. Nevertheless, the platforms were built and used for a specific application, and thus hard to reconfigure for use in other applications. A large number of LoaD diagnostic protocols are performed nowadays, and just as any laboratory has a mix of basic and specialized equipment, there are also desired basic capabilities that a general electrified platform for LoaD should ideally have. This envisaged platform should also be flexibly extendable by additional capabilities if necessary. If achieved, the right balance between modularity and specialisation will accommodate a diverse number of applications and facilitate further development of the LoaD platform. This paper reports a first version of such an open and enabling platform, and has already demonstrated its potential in several applications.

The method we present here is therefore a paradigm shift that introduces, via an embedded system, modern microsystem and microelectronic technology into the LoaD field, thereby rendering it more flexible and with a higher degree of direct interaction, for example, via a portable display device. Thus, more sophisticated concepts are possible both in the control as well as in the readout of a disc, while handling and maintenance of the system becomes easier and more reliable.

We present, in detail, each module of the eLoaD platform, and offer information specific enough for the reader to reproduce the work and adapt the system to his/her own needs. We exhibit several sensing and actuation experiments, as well as their power requirements, and detail the necessary electronic circuitry. For the sensing experiments we study optical (colorimetry) and electrochemical (with a potentiostat) detection. We further include experiments on accurate temperature readout. For the actuation experiments, we perform heating and cooling with electric components and show how to interface with the platform in real time. We provide a comprehensive list of applications for which the eLoaD platform could support diagnostic assays. The information provided in the paper is augmented by supplementary information that describes electronic schematics and programming codes, with the objective of rendering the eLoaD technology openly accessible to the community.

2. Materials and methods

2.1. The eLoaD platform: design and fabrication

The electrified Lab-on-a-Disc (eLoaD) platform was conceived to be a modular platform, on one hand to cover all the basic needs of LoaD diagnostic protocols, while on the other hand to be flexibly extendable to integrate additional capabilities. The following subsections describe essential and recurrent needs of LoaD assays, and how to fulfil them with specialised electronic modules. This reveals the concepts underlying the electrified platform, as well as its interfacing with well-established LoaD technology.

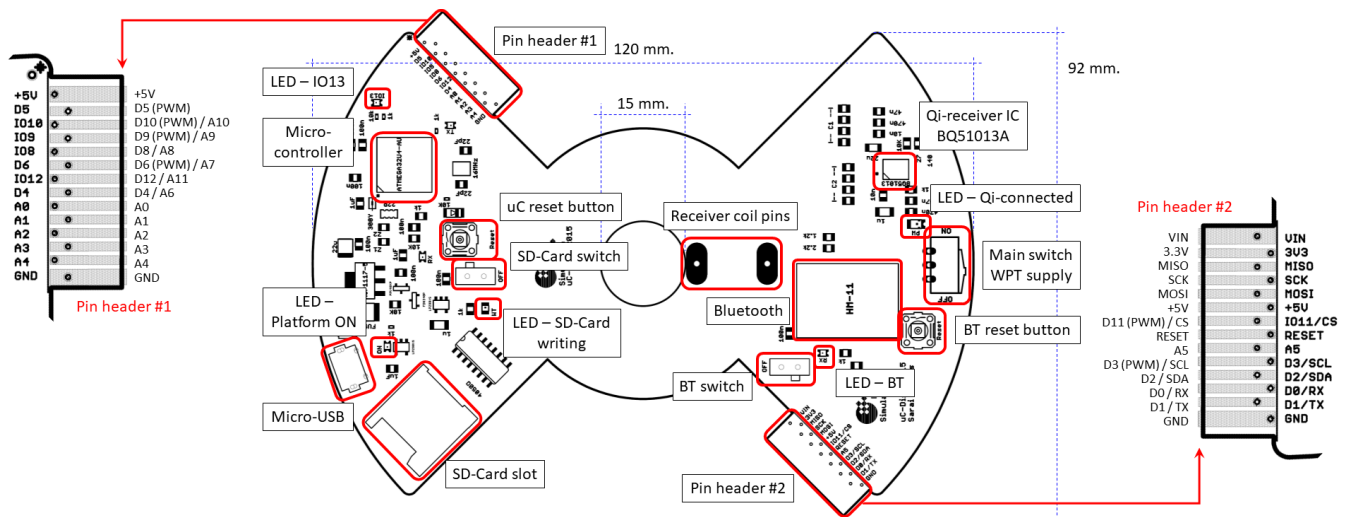


Figure 1: Layout of the eLoaD platform. The main components of each of the 4 modules are enclosed in red boundaries, including the two pin headers that provide a diversity of signal interconnects to the *ApplicationDisc*. The possible configurations of every pin are indicated. The platform has the dimensions 120 mm \times 92 mm. Its semicircular shape has a diameter of 120 mm and a hole in the center 15 mm in diameter; both measures are typical for CDs or DVDs.

2.1.1. Module I: a wireless power receiver

The first and distinguishing characteristic of the eLoaD concept is the capability to provide power to components which co-rotate with a spinning disc. Previously, different options have been presented including batteries (Boettcher et al., 2006), slip-rings (Cho et al., 1982; Martinez-Duarte et al., 2010; Abi-Samra et al., 2013), and harvesters (Joseph et al., 2015). Some of the disadvantages of these power delivery systems are the addition of weight, mechanical imbalance of the system, mechanical wear of parts, and measurement noise. With these limitations in mind, the platform was designed to comprise a Qi-compliant power receiver as a lightweight, balanced, and, importantly, reliable wireless supply of power to the rotating microfluidics experiment.

The Qi power receiver module is based on an integrated circuit BQ51013A (Texas Instruments, 2013) (located at the upper right corner in Fig. 1), and is part of the 5 W-series of Qi-compliant receivers with a 5 V output. The receiver module was designed following the guidelines of the Qi specification v1.1.2 (Wireless Power Consortium, 2016) which demands that the receiver coil is configured into a double-resonant circuit through the use of two capacitors. The purpose of the two modes is to enhance the efficiency of the transferred power (at a frequency range of 110 kHz to 205 kHz), as well as to enable the transmission of data (at a frequency of 1 MHz) at resonance. The supplementary material labelled as ‘Design of a Qi-compliant receiver’ shows the electronic schematic of this module, as well as the necessary formulae with which to calculate the values of the two capacitors for the resonance frequencies given, and relative to the inductance of the receiver coil.

Moreover, to ensure maximum power transmission, the Qi specification v1.1.2 recommends that the quality factor of the receiver coil should be higher than 77. At the same time, the receiver coil forms part of the spinning system and might therefore be subject to certain fabrication constraints. To fulfil all these geometrical and electrical requirements, we compared the characteristics obtained from coils produced under three different fabrication methods. Standard PCB fabrication was used for the first of those coils, while the second and third coils were wound using solid single strand and litz copper wires.

The receiver coil wound with a litz wire proved to have the best characteristics by far. Due to the fact that, for the three candidates, it is also the easiest to fabricate, it is our coil of choice for the receiver circuit of the platform. Nonetheless, this does not mean that other coils that fulfil the quality factor and geometrical constraints cannot be used.

Module characterisation: available power. To evaluate and ensure acceptable performance of the Qi-compliant power receiver, we measured the maximum available power at its output. Although for a centrifugal microfluidics spinstand, only the axial coil separation along the z -direction would matter (because of the ease with which to align the rotating receiver with a stationary transmitter), for completeness, we characterised power transfer also for radial misalignment to show robustness of the approach. Fig. 2 shows the maximum power available at the eLoaD platform after transmission, rectification, and regulation losses, as a function of the relative position of receiver and transmitter. Fig. 2(c) and (d) depict the available power for axial separation between the transmitter

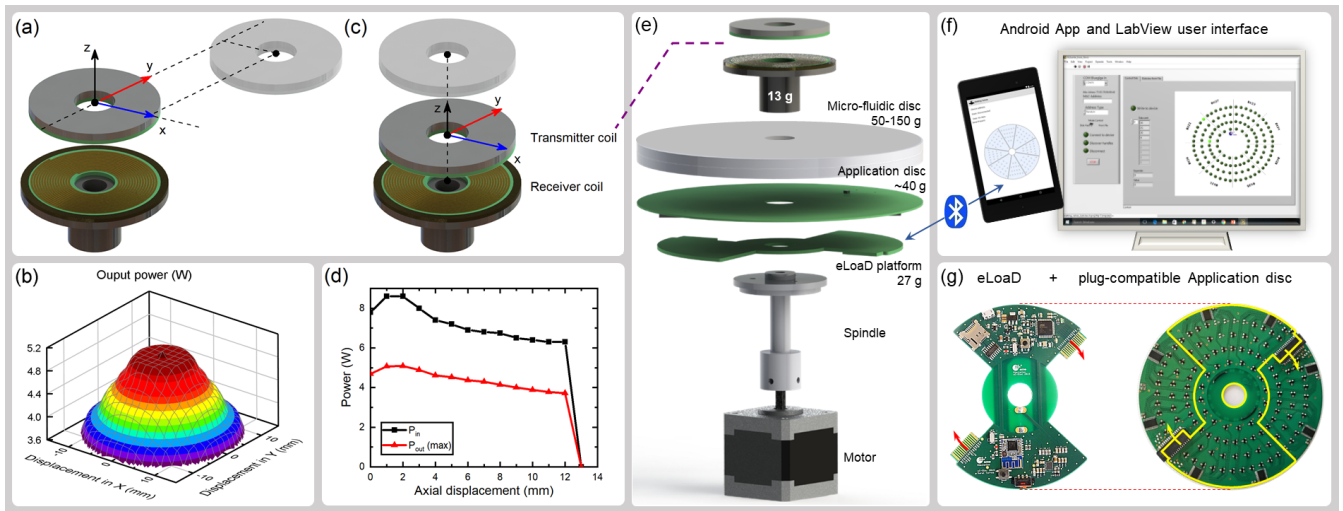


Figure 2: Maximum available power measured at the Qi-compliant power receiver's output on the eLoaD platform, evaluated for different radial $r = \sqrt{x^2 + y^2}$ (a, b) and axial z (c, d) displacements between the receiver and transmitter coils. (e) Integration of the wireless centrifugal system into conventional LoaD systems. A commercially available Qi-compliant transmitter is inductively coupled to the eLoaD platform. This fully integrated platform is able to control sensors and actuators located on the *ApplicationDisc*, which itself are simultaneously interacting with the microfluidics disc. The disposable microfluidic disc and the reusable *ApplicationDisc* are typically designed for a particular application, whereas the eLoaD platform, which implements the control logic, power, and communication, is reused as a generic framework for all possible applications. (f) Interfacing of the eLoaD platform is enabled by Bluetooth communication, here exemplarily via an Android application program running on a portable device, and from a PC running e.g. a LabVIEW script. (g) Assembly of the eLoaD platform to an *ApplicationDisc*.

and receiver. The maximum output power is obtained when the coils are placed concentrically at ≈ 2 mm separation. At this 'optimum' axial distance we measured the power available for a radial displacement from the origin, until power transmission vanished at a radial distance of ≈ 15 mm (shown in Fig. 2(a) and (b)). The highest level of power transmission was slightly above 5 W.

2.1.2. Module II: the microcontroller

The integration of a microcontroller on the platform facilitates LoaD experiments by providing control over protocol execution, increased time resolution of time-dependant detection assays, the ability to place sensors and actuators close to the sample and supply and thereby reducing convolution errors, and even allowing on-disc closed-loop control. Our choice of controller is based on the highly popular open source Arduino-micro board, which encompasses all peripherals needed to support an ATmega32U4 microcontroller (located at the upper left corner in Fig. 1). It features a built-in USB, which makes the platform recognisable to a computer by simply connecting it through a micro USB cable and enabled to be programmed with the software Arduino IDE. Fig. 1 shows two pin headers with 14 pins each that implement all the power, communication, and i/o pins. 21 of these pins can be configured as (some pins have multiple functions):

1. Digital input or output, which operate at 5 V @ 20 mA and can be used, for instance, to activate and deactivate light sources or valves (18 pins: D0-D6, D8-D12, and A0-A5).
2. Pulse-width modulated (PWM) outputs. These pins provide 8-bits of resolution to vary the duty cycle of a square signal that can be used as a pseudo-analogue output as needed, for example, for light intensity or temperature adjustment (6 pins: D3, D5, D6 and D9-D11).
3. Analogue inputs. Each of them can measure voltages coming from optical, temperature, or electrochemical sensors operating in ranges from ground (0 V) to 5 V with a resolution of 10 bits (12 pins: A0 to A11).
4. Inter-Integrated Circuit (I²C) and Serial Peripheral Interface (SPI) communication ports used by microcontrollers for rapid short distance communication with one or several peripheral devices (actuators and/or sensors in this case), all connected to only 2 to 4 lines (5 pins: SDA, SCL, MISO, MOSI and SCK).

The ATmega32U4 microcontroller operates with an external crystal oscillator of 16 MHz, this means that, for instance, a photodetector connected to an analogue input can be easily sampled at a rate in the order of tens of kilohertz, about thousand times faster than performing a discontinuous measurement with an off-disc sensor whose sampling rate would be determined by the spinning frequency, usually some tens of hertz.

2.1.3. Module III: the SD-Card

It is evident that the main objective of a diagnostic assay is to detect, to measure, and/or quantify a variable in order to provide a diagnostic result. The user should be able to record and/or transmit data for documentation, reliability, and other purposes, a task which is fulfilled by the third basic module included into the eLoaD platform, and implemented as a micro-SD breakout board (the SD-Card slot is located at the lower left corner in Fig. 1). This module is specially useful when handling large amounts of data up to 32GB.

2.1.4. Module IV: Low energy Bluetooth

For many LoaD protocols a pre-loaded recipe and a post-experimental data readout is sufficient. However, many protocols will benefit from continuous feedback, or direct interaction, while the disk is spinning. For example, depending on the actual status of a particular variable state (eg. mixing, incubation, or sedimentation), a particular action may need to be initiated based on the analyst's opinion (Torres Delgado et al., 2018). Hence it is desirable to facilitate wireless and real-time interaction with the platform and the ongoing experiment, via the implementation of a bidirectional link.

We have accommodated this by including an HM-11 Low Energy Bluetooth module (BLE 4.0) for generalised wireless communication (located at the lower right corner in Fig. 1). The module consumes about 165 mW.

Tests have been made in order to determine whether the Bluetooth connection stops working under high spinning frequencies of up to 2500 rpm, the maximum speed of our current setup, and no apparent failure has been found.

2.1.5. Physical characteristics and integration into conventional LoaD systems

Conventional LoaD spin stands are usually configured as described by Grumann et al. (2005), where a spindle motor is controlled via a software interface, and synchronised with a stroboscopic light source and a highly sensitive camera with a fast shutter. This enables high resolution stroboscopic imaging of the microfluidic disc in motion, and hence, of the liquid activity (eg. flow and mixing).

Fig. 2 shows how the eLoaD platform is integrated with this well-established technology. As depicted in Fig. 1, the size of the eLoaD platform is 120 mm × 92 mm, within a circular outline that has a diameter of 120 mm and a hole in the center of 15 mm diameter. Both dimensions are typical for CDs and DVDs, and therefore for most of the microfluidic discs. Its form factor and the headers at the board's edges enables for robustness and ease interconnection to any compatible *ApplicationDiscs* that normally will have the same size of the microfluidic discs in use. Two large pads are provided for the connection of the receiver coil. The coil can be directly attached and soldered to them, but it is provided separately in order to offer flexibility to the end user whilst configuring their own set up. To attach the receiver coil, there are two possible configurations, either below the eLoaD platform, or if spatial constraints demand it, above the entire assembly and thus connected by wires.

The light weight stack of less than 100 g formed by the eLoaD platform, connected to the *ApplicationDisc* (See Sec. 2.2) and to the receiver coil, is aligned and attached to the microfluidic disc. When all components are fastened to the motor shaft, the system is ready to spin. Moreover, to achieve wireless transmission of energy, a stationary commercial Qi-compliant Wireless Power Consortium (2016) power transmitter requires to be fixed concentrically to the motor shaft, and at the optimum distance from the receiver coil, as explained in Sec. 2.1.1. To be able to establish communication and interact with the eLoaD platform via Bluetooth, the system needs to be positioned within the range of a computer or the portable device running the user interface (for more details, please refer to Sec. 3.3).

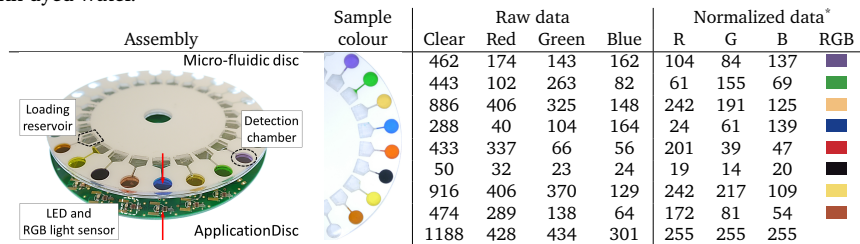
2.2. The *ApplicationDisc*

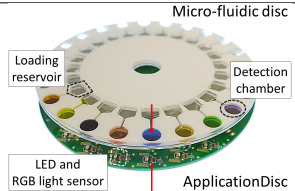
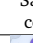
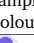








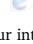

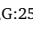
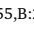


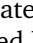
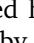
The *ApplicationDiscs* employed in our experiments are fabricated using commercially available PCB manufacturing technology, with two layers of copper, each of 35 µm in thickness, and an FR4 substrate of 1.5 mm. A few *ApplicationDisc* examples are depicted in Fig. 2(g) and Table 1, where it can be observed that the sensor and actuator elements needed for specific applications are usually placed on the top layer to be in direct contact with the microfluidic disc. The rest of components present in the circuit, needed to drive, control, amplify and/or filter data, and to interconnect it with the eLoaD platform, are located at the bottom of the disc. If elements are required on both sides of the microfluidic disc (eg. a light source in front of a detector), this can be achieved with a simple interconnection through the microfluidic disc to the *ApplicationDisc*, together with additional fixation if needed.

3. Experiments and results

In (Torres Delgado et al., 2016), we demonstrated continuous on-disc readout of a chemiluminescent signal by fitting a silicon photo-multiplier (ASD-NUV1S-P from AdvanSiD) and the necessary amplification stage circuitry (a logarithmic amplifier, LOG112 from Texas Instruments) onto an *ApplicationDisc*, showing an accuracy higher than 96% when compared to a commercial benchtop luminometer (GloMax luminometer from Promega Corporation).

Table 1: Colorimetry experiment readouts: raw and normalized data obtained from a colour light-to-digital converter (TCS3472 from TAOS-Texas Advanced Opto-electronic Solutions Inc.), placed on the top side of an *ApplicationDisc* in close and direct optical proximity to the detection chambers of a microfluidic disc placed on top. First and second columns show photographs of the disc assembly and detection chambers of the microfluidic disc filled with dyed water.



Assembly	Sample colour	Raw data				Normalized data [*]			
		Clear	Red	Green	Blue	R	G	B	RGB
		462	174	143	162	104	84	137	
		443	102	263	82	61	155	69	
		886	406	325	148	242	191	125	
		288	40	104	164	24	61	139	
		433	337	66	56	201	39	47	
		50	32	23	24	19	14	20	
		916	406	370	129	242	217	109	
		474	289	138	64	172	81	54	
		1188	428	434	301	255	255	255	

^{*} Normalization with respect to the colour intensity of a chamber filled with clear water, assuming that it corresponds to the highest intensities (white, R:255,G:255,B:255).

In (Torres Delgado et al., 2018) we demonstrated how to integrate and automate up to 128 thermally actuated valves on-disc. These were individually activated by executing a predefined timed sequence, or triggered, based on mixing and separation states, the variables being monitored in our case.

Although the use of the eLoaD platform was previously reported, a new set of simple experiments were performed to demonstrate the variety of possibilities, flexibility, and compactness that the eLoaD platform provides to LoaD experiments.

3.1. Sensing

The adequate coupling of a detector that determines the result of a LoaD experiment is critical for the automation of analytical assays. This holds true regardless of whether it depends on the detection of resistance, conductance, or capacitance changes at the active surface of an electrode (electrochemical detectors); or on a resonance frequency, or surface stress variations (mechanical detectors); or differences in the refractive index and/or light intensity, which is either generated, reflected, transmitted or absorbed (optical detectors). For sensing nearly every one of the above detectable changes of the physical properties, commercial microelectronic components exist that can be directly mounted on and read out from the *ApplicationDisc*.

3.1.1. Optical detection: colorimetry

The detection of light intensity and changes in the refractive index of a sample are key parameters for experiments that include absorbance, fluorescence, or chemiluminescence as the detection method. Without focusing on any specific assay, set of reagents, or wavelengths, the results of a simple colour detection experiment are shown in Table 1. A 12 cm diameter microfluidic disc made of multiple layers (Kinahan et al., 2014) of Poly(methyl methacrylate) (PMMA) and pressure sensitive adhesive (PSA) tape was prepared with a simple microchannel structure. Eight square reservoirs were loaded with $\approx 110 \mu\text{l}$ of dyed water (5% concentration of common food dye); a ninth reservoir was loaded with clear water to serve as a reference point. The reservoirs were each connected through separate channels to a detection chamber. The release of the samples was controlled through capillary burst valves. As the disc was accelerated, the dye water flowed through the channel and entered the circular detection chambers. Directly underneath each detection chamber, there was an opening in the bottom layer of the microfluidic disc. This opening allowed a white LED, and a colour light-to-digital converter (TCS3472 from TAOS-Texas Advanced Opto-electronic Solutions Inc.), situated on the top side of the *ApplicationDisc*, to have close and direct optical access, so as to detect and analyse the sample’s colour. The bottom side of the *ApplicationDisc* housed the rest of components needed to drive each light source and photodetector individually. The digital colour sensors are operated with 3.3 V and share a single I²C address for the communication, therefore an I²C expander was in charge of enabling and disabling each sensor and if needed, its corresponding LED.

Depending on the experimental requirements (absorbance, fluorescence or chemiluminescence detection), the platform allows to turn on the LED to illuminate the sample. Depending on the sensitivity and wavelength of interest, the light source and detector are easily replaced with suitable other components. For example, as an alternative for the white light source, a colour LED could be used, as could a laser diode with a narrower emission wavelength. For the photodetector, a photodiode with a different spectral responsivity, or higher sensitivity, could be selected as well. For example, a silicon photomultiplier such as the one used for chemiluminescence detection (Torres Delgado et al., 2018) is an option. Also, a filter could be easily accommodated.

Using the previously described setup, results were obtained after a simple normalization with respect to the colour intensity of the chamber filled with clear water (white, R:255, G:255, B:255). Although the colours did not match perfectly upon comparing the left and rightmost columns of Table 1, it is possible to achieve acceptable colour

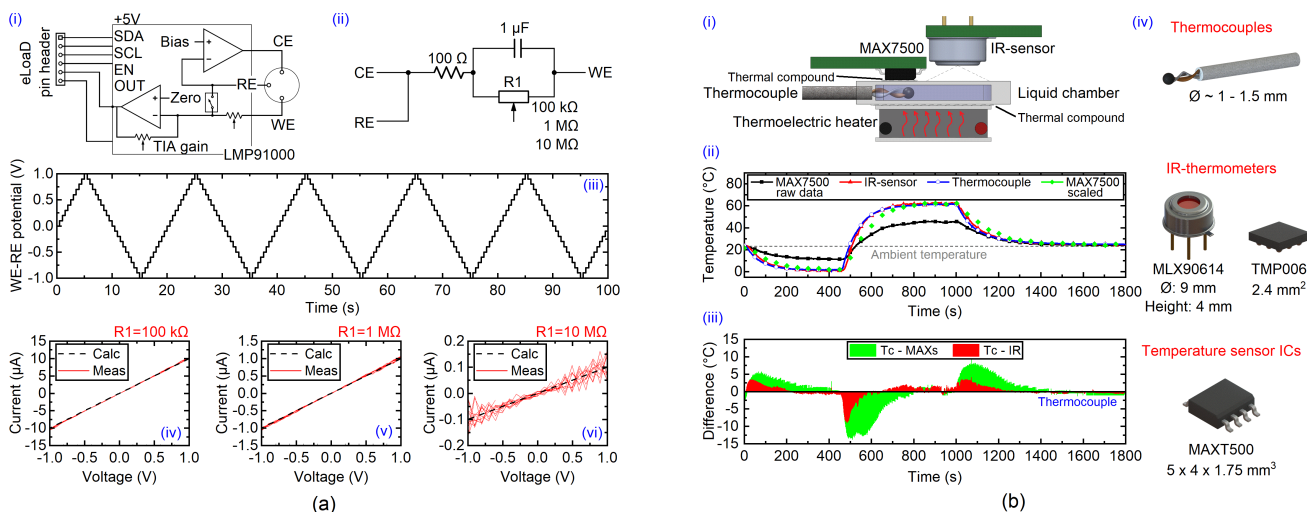


Figure 3: (a) Simple cyclic voltammetry experiment based on the (i) programmable potentiostat (LMP91000, from Texas Instruments). The pins designated for the working, counter and reference electrodes were connected to a (ii) dummy cell with three selectable impedances (working-to-reference resistance). (iii) Potential applied between the working and reference electrodes. Measured current at the working electrode for a value of R_1 of (iv) 100 k Ω , (v) 1 M Ω and (vi) 10 M Ω . (b) Temperature measurement. (i) Configuration used for the measurements. (ii) Comparison of the reaction time and raw data obtained from three different temperature sensors. The green dotted line shows how the raw data obtained from the IC temperature sensors could be compensated to obtain a read-out closer to the real value. The same colours are used to display the difference (right Y-axis) between the reference data (thermocouple temperature) and the temperatures obtained from the other two sensors. (iii) Temperature sensors utilized in this experiment. A much smaller alternative (TMP006 from Texas Instruments) to the digital plug & play infrared thermometer (MAX7500 from Maxim Integrated) is also shown.

recognition, and more importantly, light intensity data, which would be necessary for absorbance measurements. Because of the computational platform, it is conceivable to perform acceptable calibration of the system to suit the needs of a particular type of experiment, measurement condition, and the range of expected results.

3.1.2. Electrochemical detection: potentiostat

Since 1982 when rather robust setups were used (Cho et al., 1982), or with the new generation of centrifugal platforms (Kim et al., 2013) or more recently (Sanger et al., 2017), researchers have reported on electrochemical detection within a rotating platform, using slip-rings in order to not only provide power to a spinning microfluidic disc, but also to make continuous electrical contact between a peripheral potentiostat and the embedded electrodes within the disc. Here, we explored the ability to implement a compact and portable platform where not only the electrochemical cell is under rotation, embedded into the microfluidic disc, but also the necessary circuitry of a potentiostat would be mounted on the rotating platform.

For this example we selected a programmable potentiostat (LMP91000, from Texas Instruments), an IC with a $4 \times 4 \text{ mm}^2$ footprint developed for low-power chemical-sensing applications. The device itself provided all functionalities for detecting changes in current at a working electrode, and to provide at the output a voltage proportional to the cell current. Internal parameters are configurable through I²C communication, which made it convenient to interface with the eLoAD platform. These are: the potential level at which the working electrode potential should be held (“internal zero”), the potential difference between the working and reference electrodes (“bias potential”), and the transimpedance amplifier gain (“TIA gain”) for the current to voltage conversion at the working electrode.

For demonstration purposes, the pins designated for the working, counter, and reference electrodes were connected to a dummy cell (Fig. 3(a.ii)) with selectable impedance (working-to-reference resistance). Fig. 3(a.iv-v) show the measurements from a cyclic voltammetry experiment at a scan rate of 200 mV/s, fully controlled and recorded by the eLoAD platform. There is a trade-off between the simplicity and the sensitivity one could achieve with this setup. As can be observed in Fig. 3(a.iii), the minimum voltage step is 2% of the reference voltage. Also, the internal analog-to-digital converter from the microcontroller has a resolution of 10 bits ($5/1024 \text{ V}$). These issues can of course be resolved by designing a custom potentiostat circuit and by using, for instance, external ADC and DAC converters with much higher resolution than the internal devices provided by the microcontroller.

3.1.3. Temperature measurement

Even though temperature measurement is not often applied as a detection (diagnostic) method by itself, maintaining a sample at a constant temperature while performing another action (eg. sonication), heating it up (during a loop mediated isothermal amplification–LAMP), heating and cooling it down (while performing a polymerase

chain reaction–PCR) , are key steps in many assay protocols. The ability to measure a sample’s temperature in real-time is therefore often crucial. For this purpose, different options exist on the market, from simple thermistors to more sophisticated digital thermometers, which might vary in price, size, time response, and sensitivity. Here we present a comparison between an infrared (IR) thermometer (MLX90614 from Melexis, Microelectronic Integrated Systems) and a silicon based digital temperature sensor IC (MAX7500 from Maxim Integrated), taking as a point of reference the reading from a thermocouple type T in direct contact with the sample and all of which can, of course, be mounted into the rotating platform.

A difference is to be expected between the temperature take from within a sample, and that from an IC with only one of its six faces in contact with a wall of the sample chamber. Nonetheless, the measurement can be calibrated and suitably compensated to obtain a read-out close to the real value (see curves ‘MAX7500 raw data’ and ‘MAX7500 scaled’ from Fig. 3(b.ii)). Fig. 3(b.iii) shows the difference between the temperature readings. To plot this graph we considered the thermocouple readout as the reference temperature because this sensor was in direct contact with the sample. Due to the slower response time of the IR-thermometer and the IC, Fig. 3(iii) registers momentary differences up to 15 °C between the reference temperature and the readings obtained from these two external temperature sensors. Although a faster response of the IR-sensor than that of the IC is observed, the mounting and calibrating of an IC would be more convenient and flexible in most cases.

Depending on the application the sensor is being used for, the user must decide whether a fast and highly accurate response is required, or a slower and easier to mount one is sufficient. Whereas an IR-sensor would work best for thermocycling purposes, which require fast response feedback signals and drastic changes in temperature, an IC would be enough for long-time and uniform procedures, as can be when monitoring the temperature during incubation or an isothermal amplification is taking place.

3.2. Actuation

The integration of an entire lab protocol into a centrifugal disc implies not only the on-disc availability of reagents, passive components, and detectors, but frequently, active components are also needed, such as valves, or thermoelectric components, etc. Because different forms of energy movers are to be introduced into the disc, we refer to these components collectively as actuators.

3.2.1. Heating and cooling: electric components

Amplification techniques such as LAMP, recombinase polymerase amplification (RPA), or PCR, can be implemented onto a disc through the integration of thermoelectric components, to either maintain the sample at a constant temperature (LAMP), or to alternate the temperature level in defined cycles (PCR). In (Amasia et al., 2012), the authors reported a centrifugal microfluidic platform for rapid PCR amplification, integrating an off-disc thermoelectric component in close proximity to the reaction chamber for heating and cooling actions. Because of the gap between heater and the microfluidic disc, this method might result in the undesired heating of certain areas on the disc, or in the need to interrupt its motion.

The power provided by the eLoaD platform facilitates the full integration of a thermoelectric element on the *ApplicationDisc*, positioned in direct contact with the microfluidic reaction chamber. In a previous subsection we already studied the possibility of measuring temperature on-disc. Augmentation through the inclusion of a closed loop proportional-integral-derivative (PID) temperature controller for amplification purposes is readily imagined. With this end, we designed two different driving systems, the first one based on a power driver IC for Peltier elements (MAX1968 from Maxim Integrated Products), and the second one based on a high-efficiency H-bridge (DRV592 from Texas Instruments). Fig. 4 compares the measured behaviour of both driving systems in conjunction with three different actuators: a Peltier element, a ceramic heater, and a self-made Cu-Ni wire resistive heater.

For the characterisation experiment, a microfluidic disc with two different types of chambers was fabricated. A large, square-like reaction chamber ($15 \times 15 \times 2 \text{ mm}^3$) to be heated with the Peltier element and the ceramic heater, and six circular much smaller reaction chambers (of 8 mm in diameter and 2 mm in height) to be heated with the self-made resistive heater, were loaded with $\approx 500 \text{ }\mu\text{l}$ and $\approx 100 \text{ }\mu\text{l}$ of water, respectively.

As for temperature sensors, the user must decide between a fast solution with higher power consumption and more complicated control, or a slow response with simple control circuitry device, depending on the application. For example, Peltier elements are able to cool down a sample by inverting the current flow direction, providing not only a much faster decay of the temperature, but also the ability to lower the temperature below ambient, as shown in Fig. 4(a) and (b), features most likely needed while performing thermocycling. In contrast, a resistive heater with a slower time response (Fig. 4(d)) consumes less power and takes up less space on the disc. Its current path can be easily adapted to optimally cover a specific area, for example contacting several chambers at once, so that complete control over the power consumption is possible in a simple manner. These are suitable properties for long-time and uniform procedures, as when maintaining a steady temperature during incubation and isothermal

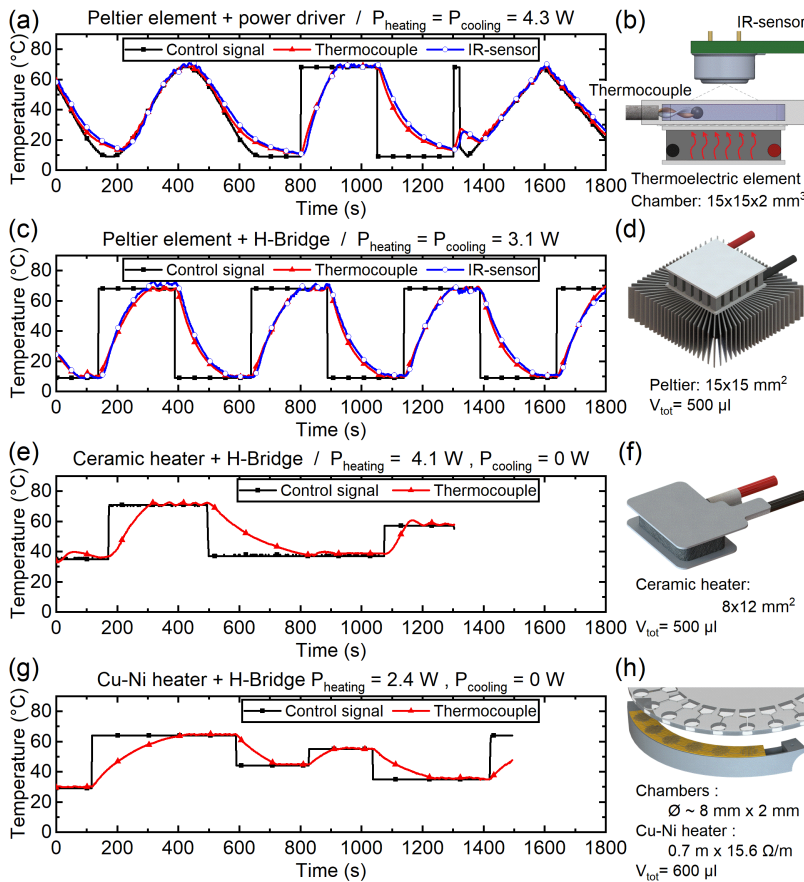


Figure 4: Comparison of the behaviour of two driving systems, and three different actuators, to achieve closed-loop control of heating and cooling. The experiment is performed with the assembly showed in (b). The control signal is plotted in black. Red and blue lines denote the temperature measured with a thermocouple and an IR sensor. Water volumes (V_{tot}) and power consumption while heating ($P_{heating}$) and cooling ($P_{cooling}$) are indicated below each actuator and above its corresponding curve. (d) Peltier element utilized in conjunction with (a) a power driver IC for Peltier elements (MAX1968 from Maxim Integrated Products), and (c) a high-efficiency H-bridge (DRV592 from Texas Instruments). (e) Curves obtained from a (f) ceramic heater driven using the H-bridge. (g) Response curves of a (h) self-made resistive heater made of Cu-Ni wire, also driven with the H-bridge.

amplification steps.

3.3. Interfacing

As alluded to in Sec. 2.1.4, the eLoaD platform includes a low energy Bluetooth (BLE 4.0) module. In our case, it allows interfacing the eLoaD platform flexibly and efficiently through a LabVIEW script running on a PC or an Android application running on a portable device. For both options, programmers are provided with a set of predefined subroutines, protocols, and tools that give access to basic functionalities, such as discovery of BLE devices within range, query of pairing, and bonding with available BLE devices (an eLoaD platform in our case), and managing the transfer of data across the link (Android 4.3 application framework (Developer Android, 2018) and BLE toolkit (National Instruments, 2017) for LabVIEW users). Fig. 2(f) shows user interfaces programmed for the activation of 128 valves, able to connect and interact with the eLoaD platform, which makes itself available by waiting for incoming connection requests. After the pairing request is accepted and the two devices exchange security keys and complete the connection process, the user can then start activating and deactivating valves either in manual or automatic control fashion as described in (Torres Delgado et al., 2018).

4. Discussion

Although small modifications and adjustments will most likely be needed, all sensing and actuation principles demonstrated before, and more, can be integrated onto and combined with the LoaD technology. These can be applied to perform other suitable concepts reported in the literature, similar for instance to the ones shown in Table 2, but now entirely on-disc and hence with dramatically improved signal-to-noise. These are in addition to the possibilities already discussed of implementing fluorescence and electrochemical detection, or the integration of heaters for amplification, sterilisation or incubation purposes. One could e.g. use any of the demonstrated heating

Table 2: Envisaged applicability of the eLoaD modules while controlling different LUOs, procedures, or entire assays, including citations to original reports.

		SD-Card	Bluetooth	Digital i/o	Analog input	PWM output	I ² C	SPI	Applicability to LUOs, procedures or entire assays
Detection	Colorimetric			✓	✓			✓	Measurement of a substance concentration in blood (Skyla, 2018; Abaxis, 2018) (eg. of glucose (Grumann et al., 2006), alcohol (Steigert et al., 2007) and liver biomarkers (albumin, total bilirubin, direct bilirubin, alkaline phosphatase, and γ -glutamyltransferase) (Nwankire et al., 2014)) or in water (LaMotte, 2018) (eg. sulphide (Kong and Salin, 2012), nitride (Czugala et al., 2013), silicate, orthophosphate and ammonium (Hwang et al., 2013)). Virus detection on lateral flow strips (Kim et al., 2014; Jung et al., 2015).
	Fluorescence*			✓	✓				Analyte detection (eg. of rat's IgG (Lai et al., 2004) or cytokine IFN- γ (He et al., 2009) using an ELISA assay and botulinum toxin (Koh et al., 2015) or vascular endothelial growth factor (Walsh Iii et al., 2014) using a bead-based fluorescence immunoassay (Riegger et al., 2006)). Nucleic acid amplification detection (eg. using PCR (Lutz et al., 2010) or RPA (Sundberg et al., 2010)).
	Chemiluminescence				✓				Analyte detection using luminescent markers (eg. bisphenol (Kubo et al., 2014) or Human C-reactive protein (CRP) (Czilwik et al., 2015; Torres Delgado et al., 2016) detection for a bead based ELISA assay).
	Electrochemical				✓		✓		Analyte detection and quantification (eg. cancer cells detection (Nwankire et al., 2012, 2015) or CRP using an ELISA assay (Kim et al., 2013), glucose concentration by using the amperometric measurement of ferricyanide ion (Cho et al., 1982; Andreasen et al., 2015; Rattanarat et al., 2015) or uric acid, and lactate levels (Li et al., 2013)). Flow analysis (eg. velocimetry (Abi-Samra et al., 2013)).
	Temperature				✓		✓	✓	Feedback signal for a closed loop thermal amplification of nucleic acids (eg. RPA (Lutz et al., 2010; Kim et al., 2014; Escadafal et al., 2014), LAMP (Jung et al., 2015) and PCR (Focke et al., 2010; Amasia et al., 2012; Burger et al., 2011; Sundberg et al., 2010; Wang et al., 2013)). Thermometric analysis.
	Imaging*			✓			✓	✓	Highly magnified visualization of flow (Grumann et al., 2005) and of the sample or a single particle fluorescence (Riegger et al., 2006; Burger et al., 2015). Colour-based analyte detection on lateral flow strips (Kim et al., 2014; Jung et al., 2015).
Actuation	Heating			✓		✓			Thermal amplification of nucleic acids (eg. RPA (Lutz et al., 2010; Kim et al., 2014; Escadafal et al., 2014), LAMP (Jung et al., 2015) and PCR (Focke et al., 2010; Amasia et al., 2012; Burger et al., 2011; Sundberg et al., 2010; Wang et al., 2013)), valving mechanism (eg. by melting wax plugs (Abi-Samra et al., 2011; Al-Faqheri et al., 2013; Park et al., 2007; Garcia-Cordero et al., 2010)) and sterilization (Chen et al., 2013).
	Cooling			✓		✓			PCR amplification (Focke et al., 2010; Amasia et al., 2012; Burger et al., 2011; Sundberg et al., 2010; Wang et al., 2013), incubation and vapor-diffusion barriers (Amasia et al., 2012).
	Valving			✓			✓		Almost any assay (eg. multistep and highly multiplexed protocols (Kinahan et al., 2014) and sequential and automated analytic procedures (Clime et al., 2015)).
	Pumping*			✓		✓			Sequential and automated analytic procedures (eg. for solid-phase extraction (SPE) of DNA (Clime et al., 2015) and rapid spectrophotometric determination (Kong and Salin, 2010, 2012)). Control of liquids (eg. through electrolysis-induced pneumatic pressure (Noroozi et al., 2011)).
	Dielectrophoresis*			✓		✓			Pumping mechanism for the control of liquids (Noroozi et al., 2011). Particle separation (Martinez-Duarte et al., 2010)).
	Data storage	✓						✓	Almost any assay (eg. recording of light intensity decay from a chemiluminescent reaction (Torres Delgado et al., 2016)).
	Interfacing		✓						Almost any assay (eg. on demand and automatic valve actuation (Torres Delgado et al., 2018)).

* Not presented here but could be implemented.

principles to perform on-disc active valving by melting wax plugs (Abi-Samra et al., 2011; Al-Faqheri et al., 2013; Park et al., 2007; Garcia-Cordero et al., 2010), expansion and contraction of trapped air chambers (Aeinehvand et al., 2015); integrate plungers on the application disc to pierce (Kinahan et al., 2016a), or deflect (Kim et al., 2016) membranes, to break internal thin walls (Aeinehvand et al., 2017), and even to press micro-channels (Cai et al., 2015, 2016); perform electrolysis-induced pumping (Noroozi et al., 2011), or mount laser diodes on the disc to enforce lysis (Kim et al., 2014).

The modularity of the eLoaD platform could play a role in facilitating the implementation of complex assays with a minimum of infrastructure. In Table 2, we consider selected papers from the LoaD literature, and classify them in terms of their measurement and automation requirements, thereby summarising some of the sensing and actuation tasks that the eLoaD could perform with only minor adaptation. Not only the reuse of the electronics platform, but also the availability of increased signal-to-noise sensors, complex actuation patterns, and real-time monitoring, add generic smart functions with little additional effort. On the other hand, standardisation of communication allows users to focus their valuable time and effort on developing the actual microfluidic assays.

5. Conclusion

This work elaborated on the complete design, fabrication, and performance, of a wirelessly connected and electrified centrifugal microfluidic system for Lab-on-a-Disc applications. Although use of the eLoaD platform was previously reported for chemiluminescence detection (Torres Delgado et al., 2016) and valving actuation (Torres Delgado et al., 2018), this paper for the first time detailed the open source hardware design forming the core of the system. Current capabilities of the platform, as well as possible future ones, were discussed in detail. The performance of the platform was characterised, demonstrating the sensing, actuating and interfacing capabilities. In particular, through the modular separation of three layers into an eLoaD microcontroller, an electronic *ApplicationDisc*, and a microfluidic LoaD, the most efficient reuse of system components and functionality could be ensured, without losing extendability of the platform for future needs.

The paper documents, in the main text and in the accompanying materials, extensive implementation details and diagrams required for producing a copy of the platform and on its proper use. It is our expressed wish to encourage the community to collaborate with us or to experiment with the eLoaD platform without barriers. In particular, we wish to support the Extreme Point of Care community (Smith et al., 2016) that aims to establish diagnostic tools for medical workers active in areas without high level primary health care. We therefore encourage interested parties to contact us at the Karlsruhe Institute of Technology in order to obtain an eLoaD platform for their own use, and to the entire community to discuss with us a redesign as an open-source hardware project that would further allow highly automated, self-calibrating, and self-testing point-of-care equipment.

Acknowledgements

This work was supported by the National Council of Science and Technology, CONACyT (Mexico), the University of Freiburg (Germany), the Karlsruhe Institute of Technology (Germany), and the European Union (H2020-FETOPEN-1-2016-2017-737043-TISuMR). The authors would like to acknowledge Prof. Dr. Ulrike Wallrabe and Prof. Dr. Jens Ducleé for providing access to their laboratories and measurement equipment at Freiburg and Dublin City Universities, respectively. We sincerely thank Dr. David Kinahan, with whom we collaborated for the already published applications, for his insight into the LoaD technique that has improved the design and applicability of our eLoaD.

Appendix A. Supplementary material

Design, fabrication, and characterisation details of the Qi-compliant receiver, as well as schematics and example codes for the implementation and use of the eLoaD's basic modules, are available in the supplementary material associated with this article that can be found in the online version at <http://dx.doi.org/....>

References

- Abaxis, 2018. Abaxis: Piccolo xpress. <http://www.abaxis.com/medical>. (accessed 16 February 2018).
- Abi-Samra, K., Hanson, R., Madou, M., Gorkin III, R.A., 2011. Infrared controlled waxes for liquid handling and storage on a CD-microfluidic platform. *Lab Chip* 11, 723–726.
- Abi-Samra, K., Kim, T.H., Park, D.K., Kim, N., Kim, J., Kim, H., Cho, Y.K., Madou, M., 2013. Electrochemical velocimetry on centrifugal microfluidic platforms. *Lab on a Chip* 13, 3253.
- Aeinehvand, M.M., Ibrahim, F., Harun, S.W., Kazemzadeh, A., Rothan, H.A., Yusof, R., Madou, M., 2015. Reversible thermo-pneumatic valves on centrifugal microfluidic platforms. *Lab Chip* 15, 3358–3369.
- Aeinehvand, M.M., Magaña, P., Aeinehvand, M.S., Aguilar, O., Madou, M.J., Martinez-Chapa, S.O., 2017. Ultra-rapid and low-cost fabrication of centrifugal microfluidic platforms with active mechanical valves. *RSC Advances* 7, 55400–55407.
- Al-Faqheri, W., Ibrahim, F., Thio, T.H.G., Moebius, J., Joseph, K., Arof, H., Madou, M., 2013. Vacuum/Compression Valving (VCV) Using Paraffin-Wax on a Centrifugal Microfluidic CD Platform. *PLoS ONE* 8, 2–10.

- Amasia, M., Cozzens, M., Madou, M.J., 2012. Centrifugal microfluidic platform for rapid PCR amplification using integrated thermoelectric heating and ice-valving. *Sensors and Actuators, B: Chemical* 161, 1191–1197.
- Andreasen, S.Z., Kwasny, D., Amato, L., Brøgger, A.L., Bosco, F.G., Andersen, K.B., Svendsen, W.E., Boisen, A., 2015. Integrating electrochemical detection with centrifugal microfluidics for real-time and fully automated sample testing. *RSC Adv.* 5, 17187–17193.
- Biosurfit, 2018. Biosurfit: SpinIt. <http://www.biosurfit.com/>. (accessed 16 February 2018).
- Boettcher, M., Jaeger, M.S., Riegger, L., Ducrée, J., Zengerle, R., Duschl, C., 2006. Lab-on-chip-based cell separation by combining dielectrophoresis and centrifugation. *Biophysical Reviews and Letters* 01, 443–451.
- Brennan, D., Coughlan, H., Clancy, E., Dimov, N., Barry, T., Kinahan, D., Ducrée, J., Smith, T.J., Galvin, P., 2017. Development of an on-disc isothermal in vitro amplification and detection of bacterial RNA. *Sensors and Actuators, B: Chemical* 239, 235–242.
- Burger, J., Gross, A., Mark, D., Stetten, F.V., Zengerle, R., Roth, G., Freiburg, D., 2011. IR thermocycler for centrifugal microfluidic platform with direct on-disk wireless temperature measurement system, in: *International Solid-State Sensors, Actuators and Microsystems Conference*, pp. 2867–2870.
- Burger, R., Amato, L., Boisen, A., 2016. Detection methods for centrifugal microfluidic platforms. *Biosensors and Bioelectronics* 76, 54–67.
- Burger, R., Kurzbuch, D., Gorkin, R., Kijanka, G., Glynn, M., McDonagh, C., Ducrée, J., 2015. An integrated centrifugo-opto-microfluidic platform for arraying, analysis, identification and manipulation of individual cells. *Lab Chip* 15, 378–381.
- Cai, Z., Xiang, J., Chen, H., Wang, W., 2016. Membrane-based valves and inward-pumping system for centrifugal microfluidic platforms. *Sens. Actuators, B* 228, 251 – 258.
- Cai, Z., Xiang, J., Wang, W., 2015. A pinch-valve for centrifugal microfluidic platforms and its application in sequential valving operation and plasma extraction. *Sens. Actuators, B* 221, 257 – 264.
- Chen, X., Song, L., Assadsangabi, B., Fang, J., Mohamed Ali, M.S., Takahata, K., 2013. Wirelessly addressable heater array for centrifugal microfluidics and Escherichia coli sterilization, in: *Annual International Conference of the IEEE Engineering in Medicine and Biology Society*, pp. 5505–5508.
- Cho, H.K., Lee, Y.H., Couch, R.A., Jagadeesh, J.M., Olson, C.L., 1982. Development of a multichannel electrochemical centrifugal analyzer. *Clinical Chemistry* 28, 1956–1961.
- Clime, L., Brassard, D., Geissler, M., Veres, T., 2015. Active pneumatic control of centrifugal microfluidic flows for lab-on-a-chip applications. *Lab Chip* 15, 2400–2411.
- Czilwik, G., Vashist, S.K., Klein, V., Buderer, A., Roth, G., von Stetten, F., Zengerle, R., Mark, D., 2015. Magnetic chemiluminescent immunoassay for human c-reactive protein on the centrifugal microfluidics platform. *RSC Adv.* 5, 61906–61912.
- Czugala, M., Maher, D., Collins, F., Burger, R., Hopfgartner, F., Yang, Y., Zhaou, J., Ducrée, J., Smeaton, A., Fraser, K.J., Benito-Lopez, F., Diamond, D., 2013. CMAS: fully integrated portable centrifugal microfluidic analysis system for on-site colorimetric analysis. *RSC Advances* 3, 15928.
- Developer Android, 2018. Bluetooth low energy: Android 4.3 (api level 18). <https://developer.android.com/guide/topics/connectivity/bluetooth-le.html>. (accessed March 2017).
- Ducrée, J., Haeberle, S., Lutz, S., Pausch, S., von Stetten, F., Zengerle, R., 2007. The centrifugal microfluidic bio-disk platform. *J. Micromech. Microeng.* 17, S103.
- Escadafal, C., Faye, O., Sall, A.A., Faye, O., Weidmann, M., Strohmeier, O., von Stetten, F., Drexler, J., Eberhard, M., Niedrig, M., Patel, P., 2014. Rapid Molecular Assays for the Detection of Yellow Fever Virus in Low-Resource Settings. *PLoS Neglected Tropical Diseases* 8.
- Focke, M., Stumpf, F., Roth, G., Zengerle, R., von Stetten, F., 2010. Centrifugal microfluidic system for primary amplification and secondary real-time PCR. *Lab on a Chip* 10, 3210.
- Focus Diagnostics, 2016. Focus diagnostics, 3m integrated cycler. <http://www.focusdx.com/integrated-cycler>. (accessed 16 February 2018).
- Garcia-Cordero, J.L., Kurzbuch, D., Benito-Lopez, F., Diamond, D., Lee, L.P., Ricco, A.J., 2010. Optically addressable single-use microfluidic valves by laser printer lithography. *Lab on a chip* 10, 2680–7.
- GenePOC, 2018. Genepoc. <http://www.genepoc-diagnostics.com/instrument/>. (accessed 16 February 2018).
- Grumann, M., Brenner, T., Beer, C., Zengerle, R., Ducrée, J., 2005. Visualization of flow patterning in high-speed centrifugal microfluidics. *Review of Scientific Instruments* 76.
- Grumann, M., Steigert, J., Riegger, L., Moser, I., Enderle, B., Riebesele, K., Urban, G., Zengerle, R., Ducrée, J., 2006. Sensitivity enhancement for colorimetric glucose assays on whole blood by on-chip beam-guidance. *Biomedical Microdevices* 8, 209–214.
- He, H., Yuan, Y., Wang, W., Chiou Nan-Rong, N.R., Epstein, A.J., Lee, L.J., 2009. Design and testing of a microfluidic biochip for cytokine enzyme-linked immunosorbent assay. *Biomicrofluidics* 3.
- Hwang, H., Kim, Y., Cho, J., Lee, J.Y., Choi, M.S., Cho, Y.K., 2013. Lab-on-a-disc for simultaneous determination of nutrients in water. *Analytical Chemistry* 85, 2954–2960.
- Joseph, K., Ibrahim, F., Cho, J., Thio, T.H.G., Al-Faqheri, W., Madou, M., 2015. Design and development of micro-power generating device for biomedical applications of lab-on-a-disc. *PLoS ONE* 10, 1–16.
- Jung, J.H., Oh, S.J., Kim, Y.T., Kim, S.Y., Kim, W.J., Jung, J., Seo, T.S., 2015. Combination of multiplex reverse-transcription loop-mediated isothermal amplification with an immunochromatographic strip for subtyping influenza A virus. *Analytica Chimica Acta* 853, 541–547.
- Kim, T.H., Abi-Samra, K., Sunkara, V., Park, D.K., Amasia, M., Kim, N., Kim, J., Kim, H., Madou, M., Cho, Y.K., 2013. Flow-enhanced electrochemical immunosensors on centrifugal microfluidic platforms. *Lab on a Chip* 13, 3747.
- Kim, T.H., Park, J., Kim, C.J., Cho, Y.K., 2014. Fully Integrated Lab-on-a-Disc for Nucleic Acid Analysis of Food-Borne Pathogens. *Analytical Chemistry* 86, 3841–3848.
- Kim, T.H., Sunkara, V., Park, J., Kim, C.J., Woo, H.K., Cho, Y.K., 2016. A lab-on-a-disc with reversible and thermally stable diaphragm valves. *Lab Chip* 16, 3741–3749.
- Kinahan, D.J., Early, P.L., Vembadi, A., MacNamara, E., Kilcawley, N.A., Glennon, T., Diamond, D., Brabazon, D., Ducrée, J., 2016a. Xurography actuated valving for centrifugal flow control. *Lab Chip* 16, 3454–3459.
- Kinahan, D.J., Kearney, S.M., Dimov, N., Glynn, M.T., Ducrée, J., 2014. Event-triggered logical flow control for comprehensive process integration of multi-step assays on centrifugal microfluidic platforms. *Lab Chip* 14, 2249–2258.
- Kinahan, D.J., Kearney, S.M., Kilcawley, N.A., Early, P.L., Glynn, M.T., Ducrée, J., 2016b. Density-gradient mediated band extraction of leukocytes from whole blood using centrifugo-pneumatic siphon valving on centrifugal microfluidic discs. *PLoS ONE* 11, 1–13.
- Koh, C.Y., Schaff, U.Y., Piccini, M.E., Stanker, L.H., Cheng, L.W., Ravichandran, E., Singh, B.R., Sommer, G.J., Singh, A.K., 2015. Centrifugal microfluidic platform for ultrasensitive detection of botulinum toxin. *Analytical Chemistry* 87, 922–928.
- Kong, L.X., Perebikovskiy, A., Moebius, J., Kulinsky, L., Madou, M., 2016. Lab-on-a-CD: A Fully Integrated Molecular Diagnostic System. *Journal*

- of Laboratory Automation 21, 323–355.
- Kong, M.C., Salin, E.D., 2012. Spectrophotometric determination of aqueous sulfide on a pneumatically enhanced centrifugal microfluidic platform. *Anal. Chem.* 84, 10038–10043.
- Kong, M.C.R., Salin, E.D., 2010. Pneumatically pumping fluids radially inward on centrifugal microfluidic platforms in motion. *Anal. Chem.* 82, 8039–8041. PMID: 20815346. <http://dx.doi.org/10.1021/ac102071b>.
- Kubo, I., Kanamatsu, T., Furutani, S., 2014. Microfluidic Device for Enzyme-Linked Immunosorbent Assay (ELISA) and Its Application to Bisphenol A Sensing. *Sensors and Materials* 26, 615–621.
- Lai, S., Wang, S., Luo, J., Lee, L.J., Yang, S.T., Madou, M.J., 2004. Design of a Compact Disk-like Microfluidic Platform for Enzyme-Linked Immunosorbent Assay. *Analytical Chemistry* 76, 1832–1837.
- LaMotte, 2018. Lamotte: Waterlink spin lab. <http://www.lamotte.com/en/pool-spa/labs/3576.html>. (accessed 16 February 2018).
- Li, T., Fan, Y., Cheng, Y., Yang, J., 2013. An electrochemical Lab-on-a-CD system for parallel whole blood analysis. *Lab on a Chip* 13, 2634.
- Lutz, S., Weber, P., Focke, M., Faltin, B., Hoffmann, J., Müller, C., Mark, D., Roth, G., Munday, P., Armes, N., Piepenburg, O., Zengerle, R., von Stetten, F., 2010. Microfluidic lab-on-a-foil for nucleic acid analysis based on isothermal recombinase polymerase amplification (RPA). *Lab on a Chip* 10, 887.
- Martinez-Duarte, R., Gorkin III, R.A., Abi-Samra, K., Madou, M.J., 2010. The integration of 3D carbon-electrode dielectrophoresis on a CD-like centrifugal microfluidic platform. *Lab on a Chip* 10, 1030.
- National Instruments, 2017. Labview ble (bluetooth low energy) toolkit. <https://forums.ni.com/t5/Community-Documents/LabVIEW-BLE-Bluetooth-Low-Energy-toolkit/tac-p/3595025#M3652>. (accessed 07 March 2018).
- Noroozi, Z., Kido, H., Madou, M.J., 2011. Electrolysis-Induced Pneumatic Pressure for Control of Liquids in a Centrifugal System. *Journal of The Electrochemical Society* 158, P130.
- Nwankire, C.E., Czugala, M., Burger, R., Fraser, K.J., Connell, T.M., Glennon, T., Onwuliri, B.E., Nduaguibe, I.E., Diamond, D., Ducreé, J., 2014. A portable centrifugal analyser for liver function screening. *Biosensors and Bioelectronics* 56, 352–358.
- Nwankire, C.E., Venkatanarayanan, A., Forster, R.J., Ducreé, J., 2012. Electrochemical Detection of Cancer Cells on a Centrifugal Microfluidic Platform. *Proceeding in ÅTAS*, 1510–1512.
- Nwankire, C.E., Venkatanarayanan, A., Glennon, T., Keyes, T.E., Forster, R.J., Ducreé, J., 2015. Label-free impedance detection of cancer cells from whole blood on an integrated centrifugal microfluidic platform. *Biosensors and Bioelectronics* 68, 382–389.
- Park, J.M., Cho, Y.K., Lee, B.S., Lee, J.G., Ko, C., 2007. Multifunctional microvalves control by optical illumination on nanoheaters and its application in centrifugal microfluidic devices. *Lab on a Chip* 7, 557.
- Rattanarat, P., Teengam, P., Siangproh, W., Ishimatsu, R., Nakano, K., Chailapakul, O., Imato, T., 2015. An Electrochemical Compact Disk-type Microfluidics Platform for Use as an Enzymatic Biosensor. *Electroanalysis* 27, 703–712.
- Riegger, L., Grumann, M., Nann, T., Riegler, J., Ehlert, O., Bessler, W., Mittenbuehler, K., Urban, G., Pastewka, L., Brenner, T., Zengerle, R., Ducreé, J., 2006. Read-out concepts for multiplexed bead-based fluorescence immunoassays on centrifugal microfluidic platforms. *Sensors and Actuators, A: Physical* 126, 455–462.
- Samsung, 2017. Samsung: Labgeo ib10. <http://www.samsung.com/global/business/healthcare/healthcare/in-vitro-diagnostics/BCA-IB10/DE>. (accessed 16 February 2018).
- Sanger, K., Zór, K., Bille Jendresen, C., Heiskanen, A., Amato, L., Toftgaard Nielsen, A., Boisen, A., 2017. Lab-on-a-disc platform for screening of genetically modified *E. coli* cells via cell-free electrochemical detection of p-Coumaric acid. *Sensors and Actuators, B: Chemical* 253, 999–1005.
- Skyla, 2018. Skyla: Vb 1: Veterinary clinical chemistry analyzer. <http://www.skyla.com/index.aspx>. (accessed 16 February 2018).
- Smith, S., Mager, D., Perebikovskiy, A., Shamloo, E., Kinahan, D., Mishra, R., Torres Delgado, S.M., Kido, H., Saha, S., Ducreé, J., Madou, M., Land, K., Korvink, J., 2016. CD-Based Microfluidics for Primary Care in Extreme Point-of-Care Settings. *Micromachines* 7, 22.
- SpinChip Diagnostics AS, 2018. Spinchip diagnostics as. <http://www.spinchip.no/>. (accessed 16 February 2018).
- Steigert, J., Brenner, T., Grumann, M., Riegger, L., Lutz, S., Zengerle, R., Ducreé, J., 2007. Integrated siphon-based metering and sedimentation of whole blood on a hydrophilic lab-on-a-disk. *Biomedical Microdevices* 9, 675–679.
- Strohmeier, O., Keller, M., Schwemmer, F., Zehnle, S., Mark, D., von Stetten, F., Zengerle, R., Paust, N., 2015. Centrifugal microfluidic platforms: advanced unit operations and applications. *Chem. Soc. Rev.* 44, 6187–6229.
- Sundberg, S.O., Wittwer, C.T., Gao, C., Gale, B.K., 2010. Spinning disk platform for microfluidic digital polymerase chain reaction. *Analytical Chemistry* 82, 1546–1550.
- Texas Instruments, 2013. Texas instruments bq51013a datasheet. <http://www.ti.com/lit/ds/symlink/bq51013a.pdf>. (accessed July 2016).
- Torres Delgado, S.M., Kinahan, D.J., Nirupa Julius, L.A., Mallette, A., Ardila, D.S., Mishra, R., Miyazaki, C.M., Korvink, J.G., Ducreé, J., Mager, D., 2018. Wirelessly powered and remotely controlled valve-array for highly multiplexed analytical assay automation on a centrifugal microfluidic platform. *Biosensors and Bioelectronics*.
- Torres Delgado, S.M., Kinahan, D.J., Suárez Sandoval, F., Nirupa Julius, L.A., Kilcawley, N.A., Ducreé, J., Mager, D., 2016. Fully automated chemiluminescence detection using an electrified-lab-on-a-disc (eload) platform. *Lab Chip* 16, 4002–4011.
- Walsh Iii, D.I., Sommer, G.J., Schaff, U.Y., Hahn, P.S., Jaffe, G.J., Murthy, S.K., 2014. A centrifugal fluidic immunoassay for ocular diagnostics with an enzymatically hydrolyzed fluorogenic substrate. *Lab on a chip* 14, 2673–80.
- Wang, G., Ho, H.P., Chen, Q., Yang, A.K.L., Kwok, H.C., Wu, S.Y., Kong, S.K., Kwan, Y.W., Zhang, X., 2013. A lab-in-a-droplet bioassay strategy for centrifugal microfluidics with density difference pumping, power to disc and bidirectional flow control. *Lab on a Chip* 13, 3698.
- Wireless Power Consortium, 2016. Wpc qi specification version 1.2.2. <https://www.wirelesspowerconsortium.com/downloads/download-wireless-power-specification.html>. (accessed December 2017).